

Flow Transition in the Wake of a Rotating Sphere

C.J. Pregalato¹, M.C. Thompson¹ and K. Hourigan¹

¹Department of Mechanical Engineering
Monash University, Clayton, Victoria, 3800 AUSTRALIA

Abstract

The flow past a rotating sphere is investigated numerically using a three-dimensional spectral element/spectral direct numerical simulation. The effect of sphere rotation on transition regimes is analysed for Reynolds numbers of $10 < Re < 500$, where Re is the Reynolds number based on freestream velocity U , sphere diameter d and kinematic viscosity ν . The results show that the Reynolds numbers for the first transition to three-dimensionality, Re_1 , and the second transition to time-dependence, Re_2 , are functions of the angular velocity of the sphere Ω (normalised by the sphere radius and freestream velocity). The effect of non-streamwise sphere rotation is to reduce the critical Reynolds numbers at which transition first occur. However, rotation about the streamwise axis results in a delayed transition, due to the suppression of the out-of-plane velocity component which is thought to trigger the flow transition.

Introduction

Rotating spheres are important in many industries, such as mineral processing, environmental protection and sports. For example, particle-laden and suspension flows are widely encountered in production, and therefore it is of great practical interest to investigate particle motion in designing manufacturing equipment. The present study aims to explore the impact of rotation on the transition Reynolds numbers for a sphere rotating about the streamwise and non-streamwise axes respectively.

Previous investigations of the motion of a spinning sphere have mainly dealt with small particle Reynolds numbers, namely Re_p much less than unity. However, in recent years experiments have been performed on the lift of spinning spheres at intermediate Re . Oosterle and Bui Dinh [5] looked at Reynolds numbers less than 140, and proposed an empirical expression to estimate the lift coefficient within this range and for dimensionless angular velocities varying from 1 to 6. In spite of this, they could not explain the behaviour of the lift coefficient in terms of Re and Ω and acknowledge that further information is required concerning the flow structure around the sphere.

A three-dimensional finite difference scheme based on the marker-and-cell technique was used by Kurose and Komori [4] to perform computations of the flow around a rotating sphere in a linear shear flow. The rotation rates investigated were in the range $0 < \Omega < 0.25$, whereas the Reynolds number ranged from 1 to 500. In this study, it was found that the drag increases with increasing rotation. Also, the sign of the lift coefficient remains unchanged with increasing Re in contrast to a fixed sphere in a linear shear flow, and approached a constant value for $Re > 200$ for a given rotational speed. This asymptotic value of the lift coefficient increased with increasing rotation rate, as did the Strouhal number St . Expressions for lift and drag were proposed for the parameter range investigated.

Johnson and Patel [2] analysed in detail the transition processes between flow regimes in the wake of a fixed sphere. They postulate that the first transition is associated with an azimuthal instability of the low-pressure core of the toroidal vortex. The previously closed separation bubble opens up due to the azimuthal pressure gradient and entrains fluid through two tails. This mechanism is extended to describe the transition to unsteadiness.

The nature of the transitions in the wake of a stationary sphere has been studied extensively in the literature. Thompson *et al.* [6] constructed Landau models for both Re_1 and Re_2 and suggest that the first transition is due to the tilting of fluid rings as they pass close to the surface of the sphere, thus converting azimuthal vorticity into streamwise vorticity. A precursor for the second transition is kinking of the counter-rotating vortices at approximately one diameter downstream of the sphere. However, further information is required concerning the characteristics of this transition.

Numerical Procedure

A spectral element/spectral numerical method developed for axisymmetric geometries was used for flow computations. The (dimensionless) Navier-Stokes and continuity equations are written with respect to polar coordinates and are solved using a high-order, three-step time-splitting scheme proposed by Karniadakis *et al.* [3]. Singularities caused by the polar transformation are removed before application of the variational projection, as described in Tomboulides *et al.* [9]. Because of the inherent periodicity of 2π in the azimuthal direction, a conventional Fourier interpolation is used to analyse the flow in its m Fourier modes in three dimensions. This technique has been applied successfully in studying the flow regimes of a cylinder wake. Further details of the method may be found in Thompson *et al.* [7].

Results

Grid Resolution Study

An extensive study was performed to investigate the change in solution caused by varying the grid parameters. The mesh used for the calculations had 107 conforming quadrilateral elements with 24 Fourier planes and is shown in figure 1. The dimensions of the mesh in terms of the sphere diameter are as follows: outlet (L_O), 12.5; inlet (L_I), 15; radial (L_R), 15. Results computed on this mesh have been examined for convergence by changing the order of the tensor-product Lagrange polynomial interpolants used for the primitive variable expansions.

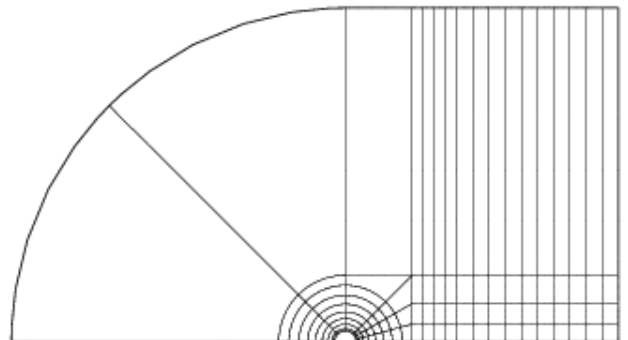


Figure 1. 2-D spectral element mesh used for all simulations.

N	6	7	8	9	10
St	0.1348	0.1346	0.1341	0.1338	0.1340
C_D	0.6435	0.6476	0.6492	0.6510	0.6512
C_L	0.0602	0.0610	0.0618	0.0622	0.0622
$u(2,0.5)$	0.9715	0.9786	0.9824	0.9876	0.9869

Table 1. Convergence results for a fixed sphere, where N is the order of the Lagrange polynomial interpolant used in each element.

Table 1 shows the global Strouhal number, drag and lift coefficients, as well as velocity fluctuations measured in the wake at a point 2 diameters downstream of the fixed sphere and located close to the separated shear layer. The difference in solution between $N = 8$ and $N = 10$ is less than 1%, and all subsequent calculations use $N = 8$ as the basis for the interpolating polynomials.

For a finite domain mesh, blockage effects become important and were analysed using a further two meshes, one with twice the radial extent as the primary mesh and the other with half the radial extent. Although not presented here, it was found that the change in solution between the primary and the large mesh was negligible, whereas the difference between the primary and the small mesh was in the order of 5%. The outcome of increasing L_O to 25 and 50 diameters also resulted in little difference, and the vortical structures emanating from the rear of the sphere at higher Re did not seem to be affected by the shorter outlet length used in the primary mesh.

Rotating Sphere Computations

Simulations were performed for the rotating sphere for Reynolds numbers in the range $10 < Re < 500$ and sphere angular velocities varying from $0.05 < \Omega < 0.25$. Although rotations about all three primary axes were performed, the results presented herein concern only x - and z -axis rotations, since rotations about the y -axis yielded essentially identical outcomes as the z -axis rotations due to the nominal two degree-of-freedom representation of the boundary conditions on the surface of the sphere.

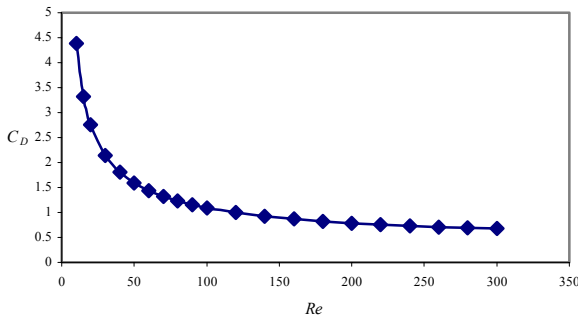


Figure 2. Drag coefficient for $\Omega = 0.10$.

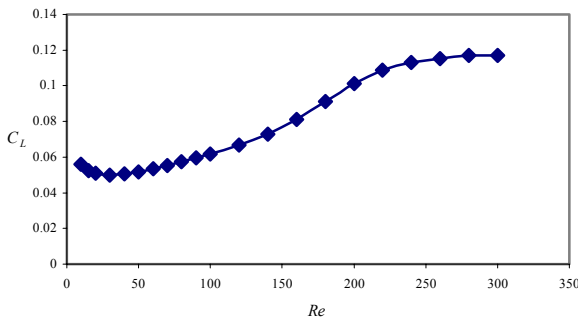


Figure 3. Lift coefficient for $\Omega = 0.10$.

Although plots of velocity vectors, streamlines and vorticity contours do much to understand the dynamics of the wake, they do not clearly elucidate the wake structures as observed in experiments. Hence, vortex structures were computed in the post-processing phase of the calculations by determining and plotting isosurfaces of $-\lambda_2$, which is the second eigenvalue of the $\mathcal{S}^2 + \mathcal{Q}$ tensor, where \mathcal{S} and \mathcal{Q} are the symmetric and antisymmetric components of the velocity gradient tensor. This method has been widely used in visualising vortex structures in a variety of flows, as reported by Jeong and Hussain [1].

For all rotation rates investigated, it was found that both the drag and lift forces increased with increasing Ω at any given Reynolds number. Furthermore, the drag coefficient at a given rotation rate exhibited similar behaviour to that of a stationary sphere: C_D rapidly decreases with increasing Re , as shown in figure 2. The lift coefficient, on the other hand, initially decreased with Re and then roughly increased linearly to a maximum value at a Reynolds number which is relatively independent of the rotation rate. This maximum value of lift remains virtually unchanged for the higher Re investigated in this study and is depicted in figure 3. A similar trend was observed by Kurose and Komori [4]. For $Re \geq 240$, the flow was found to be unsteady and hence the values for lift and drag depict time-averaged quantities. However, it should be noted that for rotation about the streamwise axis, both lift and side (lateral) forces were zero up to Reynolds numbers of ≈ 280 , due to the axisymmetric nature of the flow at these conditions.

An analysis of the vortical structures in the wake reveals that the levelling out of the lift coefficient at $Re > 240$ corresponds to the onset of periodic vortex shedding in the form of vortex loops or “hairpin” vortices. For the case of a stationary sphere, this regime is encountered only for $Re > 275$, according to the present results. For a stationary (nonrotating) sphere, the flow remains steady and axisymmetric up to a Reynolds number of approximately 212. However, for a non-streamwise-rotating sphere, the axisymmetry is broken by the component of velocity in the plane orthogonal to the axis of rotation, even at the relatively low Reynolds numbers investigated in this study. For example, an examination at $Re = 10$ found the flow to be very slightly nonaxisymmetric, but not unstable enough to induce transition to the double-thread wake.

Not only does the out-of-symmetry-plane velocity component break the axisymmetry, it is also responsible for the orientation of the plane of symmetry (see figure 4). For a fixed sphere, the plane of symmetry in the steady, nonaxisymmetric wake is known to be arbitrary, whereas for a rotating sphere it is found to be dependent upon the direction of rotation. Furthermore, the evolution of the dual counter-rotating vortices as shown in figure 4 seems to be related to this same velocity component as the fluid develops more inertia at higher Reynolds numbers, and lends weight to the conjecture proposed by Johnson and Patel [2] and advanced by Thompson *et al* [6]. Indeed, at $Re_1 \approx 100$ and an angular rotation of 0.05, the flow was unstable enough to promote the development of the well-known double-thread wake. However, this transition process requires more information regarding the time evolution of the wake as it changes to a different flow state.

The second transition to unsteadiness occurs at $Re_2 \approx 240$, for a non-streamwise rotation of $\Omega = 0.05$. The vortex structures at this Reynolds number are shown in figure 4, and depict the well-known hairpin vortex configuration (see, for example, [2]), although somewhat demarcated due to the rotational nature of the flow.

For the streamwise-rotating sphere, the breakdown of axisymmetry was observed at $240 < Re_1 < 260$, with an angular rotation of $\Omega = 0.10$. A plot of the vortex structures in this regime is shown in figure 5. Clearly evident is the difference in strength of the two counter-rotating vortices, more noticeable in the

bottom view of figure 5. This is because the (streamwise) angular velocity in the wake induced by the rotating sphere is in the same direction as one of the counter-rotating vortices, and in the opposite direction of the other. Hence, one of the vortices increases in strength whereas the other diminishes due to the termination of streamwise vorticity. The rotation also causes the two tails to be slightly skewed about the streamwise axis. The delayed transition in the case of the streamwise-rotating sphere is once more related to the out-of-symmetry-plane velocity, as this is the component of velocity that is subdued rather than promoted, as is the case with non-streamwise rotations. The difference in strength between the counter-rotating vortices results in a flow field that is quite unstable. Whereas $Re_2 \approx 240$ for non-streamwise rotation, for a streamwise rotating sphere the transition Reynolds number lies in the range $280 < Re_2 < 300$ for $\Omega = 0.10$.

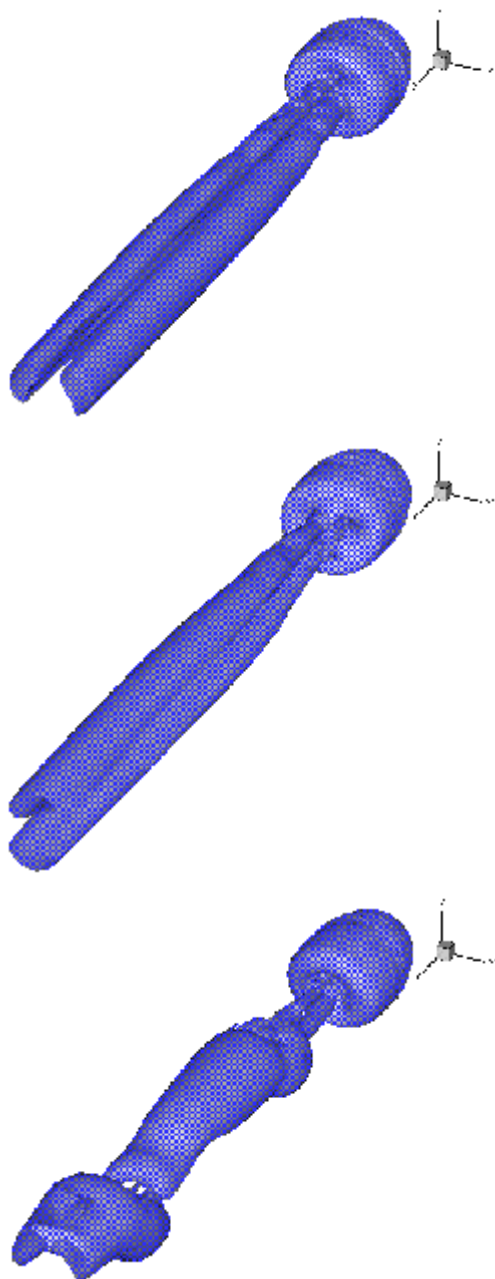


Figure 4. Rotating sphere about the y (top) and x (middle) axes respectively, $Re = 200$. Bottom view: $Re = 260$, $\Omega_y = 0.05$.

The relatively short Reynolds number range in which the double-thread wake is observed for a streamwise rotating sphere appears to be related to the large increase in entrained streamwise vorticity. For example, the difference in strength of the counter-rotating vortices between $260 < Re < 280$ was visually evident, while the same difference in Re for a non-streamwise rotating sphere generated vortices whose relative strength was barely discernible.

For a stationary sphere, the transition to non-axisymmetry is evidenced by the occurrence of two counter-rotating vortices. Although the wake is asymmetric, there still exists a plane of symmetry, and the two-tailed wake structure often observed in experiments is a result of the conversion of azimuthal vorticity into streamwise vorticity. Because the azimuthal velocity in the wake is zero prior to transition, it provides a useful means of calculating the Reynolds number at which transition occurs.

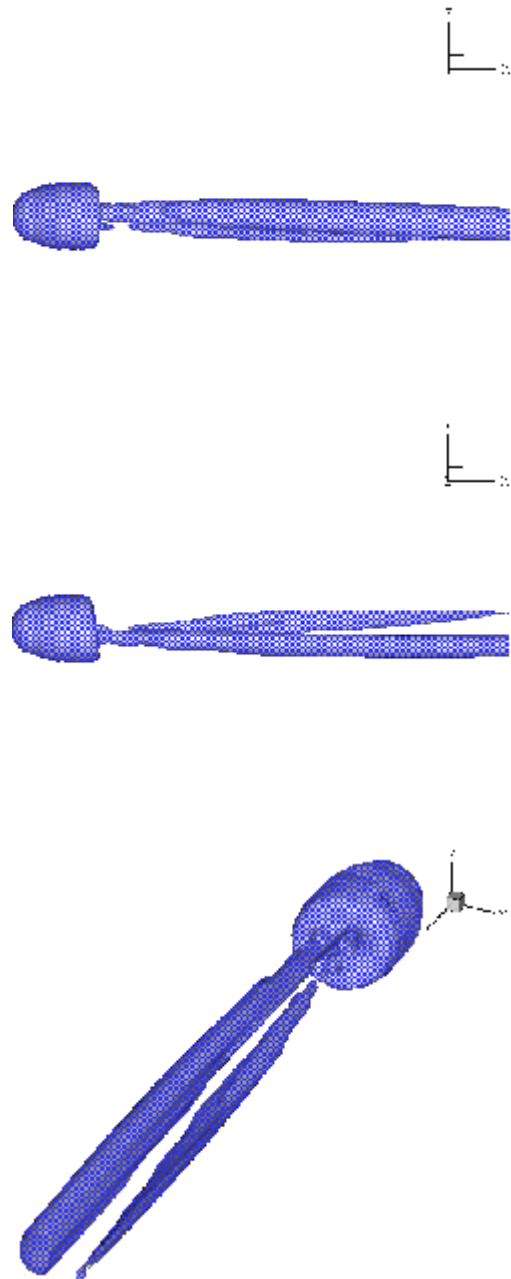


Figure 5. Rotating sphere about the x -axis, $Re = 260$.

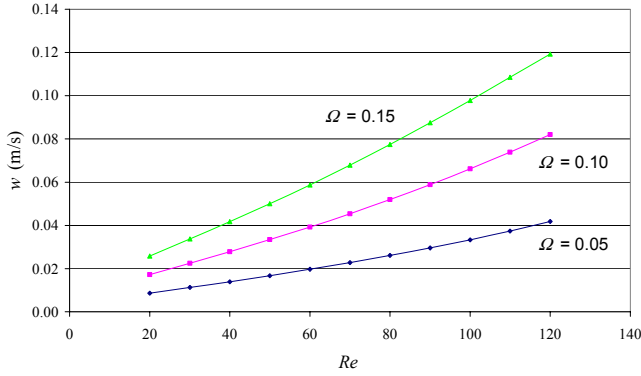


Figure 6. Azimuthal velocity at a location $(x,y,z) = (4.5,0,0)$.

However, for a rotating sphere, the azimuthal velocity at an arbitrary point in the wake is not zero, and hence makes it difficult to identify transition. Furthermore, in contrast to the flow past a stationary sphere, the azimuthal velocity cannot be used to identify the initial occurrence of the two-tailed wake structure. Figure 6 depicts the azimuthal velocity for a (non-streamwise) rotating sphere as a function of Re , obtained at a position two diameters immediately downstream of the sphere. Quite apparent is the linear nature of the non-zero velocity fluctuations, even in the neighbourhood of the occurrence of the two-tailed vortex structure, whose values are shown in Table 2. The numerical simulations demonstrate that even at the low Reynolds numbers investigated in this study, considerable streamwise vorticity was observed in the wake, although the flow was non-axisymmetric and a two-tailed structure was not evident. Moreover, it appears that as the streamwise vortices grow in strength (to a magnitude comparable to that of a stationary sphere immediately after transition), the mutual force exerted by the counter-rotating vortices is considerable enough to disperse the vortices away from the wake centre plane, and yields the two-tailed structure observed in the numerical simulations and well documented in experiments.

Angular rotation (Ω)	Observed two-tailed wake Re
0.05	95 ± 5
0.10	55 ± 5
0.15	45 ± 5
0.20	35 ± 5
0.25	25 ± 5

Table 2. Reynolds numbers at which two-tailed wake structure is observed.

Simulations were performed at Reynolds numbers of 350, 400, 450 and 500 for $\Omega_x = 0.10$ and $\Omega_y = 0.05$. At all of these Re , although not presented here, time histories of velocity fluctuations measured 2 diameters downstream revealed a somewhat random character, comparable to the wake pattern observed by Tomboulides and Orszag [8] in their figures 18 and 19. Although the wake is to some extent chaotic, there is to be expected a pronounced peak in the Strouhal number at the vortex shedding frequency, as well as smaller peaks corresponding to the loss of planar symmetry, etc. However, some descriptive quantities used to characterise the wake properties (such as Strouhal numbers) are dependent upon the position in the wake where they are measured, and averaging is required in order to make comparisons with complementary results. Further work will investigate the spectral characteristics of the flow at these higher Reynolds numbers.

Conclusions

The flow about a rotating sphere was analysed numerically using a three-dimensional spectral element/spectral method for axisymmetric geometries. It was found that a non-streamwise sphere rotation caused an earlier transition to non-axisymmetry, whereas a streamwise rotation resulted in a greatly delayed transition in relation to the Reynolds number. The orientation of the plane of symmetry as well as the transition to non-axisymmetry are related to the out-of-symmetry-plane velocity component. An increase in sphere rotation resulted in an increase in both drag and lift for any given Re , however, further information is required regarding the nature of the transitions.

Acknowledgments

This work was supported by the Australian Research Council. The first author would like to acknowledge support provided through a Monash Departmental Scholarship.

References

- [1] Jeong, J. & Hussain, F., On the identification of a vortex, *J. Fluid Mech.*, **285**, 1995, 69-94
- [2] Johnson, T.A. & Patel, V.C., Flow past a sphere up to a Reynolds number of 300, *J. Fluid Mech.*, **378**, 1999, 19-70.
- [3] Karniadakis, G.E., Israeli, M. & Orszag, S.A., High-order splitting methods for the incompressible Navier-Stokes equations, *J. Comput. Phys.*, **97**, 1991, 414-443.
- [4] Kurose, R. & Komori, S., Drag and lift forces on a rotating sphere in a linear shear flow, *J. Fluid Mech.*, **384**, 1999, 183-206.
- [5] Oesterle, B. & Bui Dinh, T., Experiments on the lift of a spinning sphere in a range of intermediate Reynolds numbers, *Exp. Fluids*, **25**, 1998, 16-22.
- [6] Thompson, M.C., Leweke, T. & Provansal, M., Kinematics and dynamics of sphere wake transition, *J. Fluids Struct.*, **15**, no. 3-4, 2001, 575-585.
- [7] Thompson, M.C., Hourigan, K. & Sheridan, J., Three-dimensional instabilities in the wake of a circular cylinder, *Exp. Therm. Fluid Sci.*, **12**, 1996, 190-196.
- [8] Tomboulides, A.G. & Orszag, S.A., Numerical investigation of transitional and weak turbulent flow past a sphere, *J. Fluid Mech.*, **416**, 2000, 45-73.
- [9] Tomboulides, A.G., Orszag, S.A. & Karniadakis, G.E., Direct and large eddy simulations of axisymmetric wakes, *AIAA paper 93-0546*, 1993.